

# COMPUTATION OF OVERVOLTAGES USING ELECTROMAGNETIC FIELD APPROACH DURING BACK-TO-BACK CAPACITOR SWITCHING OPERATIONS IN A SUBSTATION

W. RUAN, F. P. DAWALIBI, S. FORTIN, J. MA  
Safe Engineering Services & technologies ltd.  
1544 Viel, Montreal, Canada, H3M 1G4  
Email: info@sestech.com Web: www.sestech.com

**Abstract:** *A new technique to model switching operations in the frequency domain using electromagnetic field theory has been developed and applied to study the transient voltages developed due to capacitor bank switching in a system involving both aboveground and buried conductors. The computed transient voltage is in reasonable agreement with measurements. This value is also compared with the one obtained by a hybrid method<sup>1</sup>.*

## 1. Introduction

Capacitor bank switching operations in a substation often lead to high transient voltages developed at the capacitor banks and in the grounding grid of the substation. These voltages can damage equipment, particularly sensitive electronics, and thus represent a significant operating cost. The study of transient currents and voltages due to capacitor switching is a complex one. The outcome of the switching event depends on a number of parameters such as: the status of the capacitor banks at the moment of switching, the configuration of the network under study, the switching time and time delays between phase switching. There are also theoretical difficulties caused by the fact that transient phenomena of this kind are both time-dependent and frequency-dependent<sup>1</sup>.

Several approaches could be used to overcome these difficulties. One could, for instance, attempt to model the switching in the frequency domain and solve the complete network in the frequency domain with the help of Fourier transforms. Another possibility would be to try to represent the frequency dependence of the conductor properties as an equivalent time dependence and then solve the complete network directly in the time domain. While both of these approaches are possible, they are time-consuming and very complex.

This paper presents a study conducted to analyze the transient voltages and currents developed during capacitor bank switching operations at a typical substation. In a previous study<sup>1</sup>, the authors have used a hybrid method in which both frequency-based and time-based solutions are obtained and combined. This computation method reproduces the main features of the high transient voltages observed at the substation.

In this paper, the conductor network is analyzed and solved completely in the frequency domain using a new technique to model the switching operation in the frequency domain. The transient voltages and currents due to the capacitor bank switching are then obtained by Fourier transforms. The computation results are compared to measurements and also to the results obtained previously using the hybrid method. For the completeness of this paper and convenience of the reader, the sections entitled "Description of The Physical System" and "Experiment Results" in Ref. 1 have been included here, with small modifications to suit this paper.

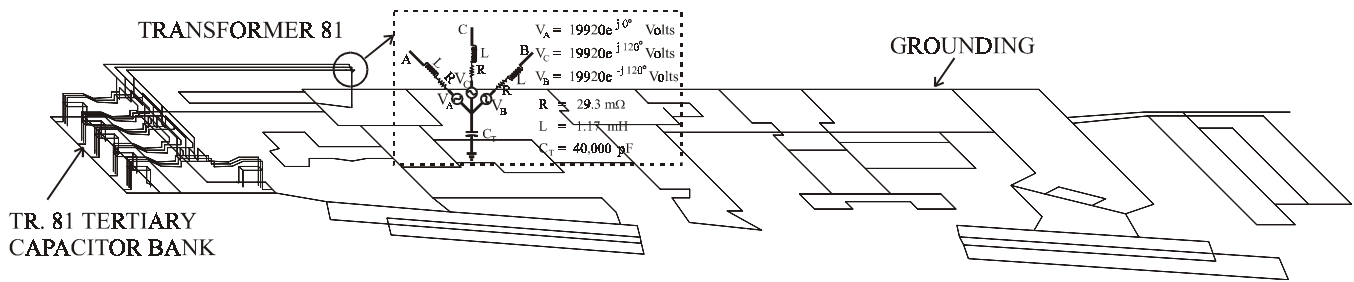
## 2. Description of the Physical System

Figure 1 shows the substation that was modeled for this study. It includes a substantial portion of the grounding system, the secondary side of a transformer, a set of six capacitor banks and the bus work connecting them to the transformer. The grounding system of the substation covers an area of about 300 by 600 feet.

The aboveground bus work consists of L-shaped main bus feeders fed by a 345/138/34.5 kV auto-transformer, as well as a set of secondary bus bars feeding the capacitor banks (see Figure 2). The auto-transformer tertiary winding is delta-connected and has a 34.5 kV rating of 108 MVA and a winding capacitance to ground of 40,000 pF. To simplify the modeling, this was represented as an equivalent ungrounded Y-connected system (Inset of Figure 1). Each branch contains an ideal voltage source of  $34,500 / \sqrt{3} = 19,920$  Volts in series with an inductance of 1.17 mH and a resistance of 29.3 m $\Omega$ , which represents a Thevenin equivalent for the transformer. The resistance was obtained by assuming an X/R ratio of 15. It must be emphasized that these impedance values are valid for a 60 Hz signal; in particular, the resistance can be considerably greater at higher frequencies.

The neutral of the Y-connection was physically connected to the grounding system through a lumped capacitance of 40,000 pF to represent the tertiary winding capacitance to ground.

A simplified model was used for the capacitor banks. Each phase wire is connected to a lumped capacitance of 43.84  $\mu$ F. The enclosure of the capacitor banks is connected to the grounding system at two points, as shown in Figure 2. This provides a low impedance path for the current to flow between the capacitor banks.



**Figure 1. Modeled Area of the Substation**

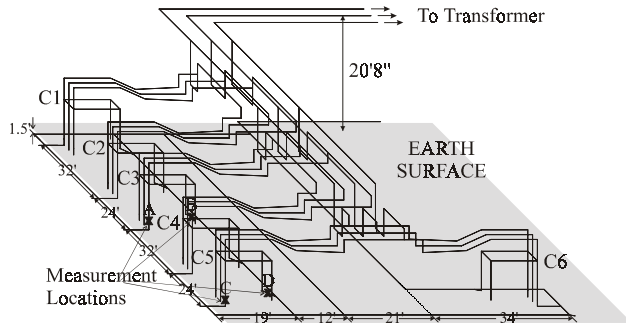


**Figure 2. Transformer 81 Tertiary Capacitor Bank System and Locations of Measurement**

### 3. Experimental Results

Experiments were conducted by Commonwealth Edison personnel<sup>1</sup> to characterize the nature of the switching transients.

The experiments measured the potential difference between points on Capacitor Banks 81-C3 and 81-C5 and a wire connected to a 120 V source grounded to a point located on the same grid as the capacitor banks, about two hundred feet away from them. The measurement points are identified as A, B, C, and D in Figure 2. Several events were studied.

Figure 3 shows the measurement results for a typical event, Event #16, which corresponds to switching on Capacitor Bank 81-C5, with Capacitor Bank 81-C3 already in service. The measurement location corresponds to Point B.

Figure 3(a) shows the measurement results for Event #16 over one period of the reference source signal. Two very sharp peaks are clearly visible. The first peak has a peak-to-peak amplitude of about 1000 Volts and the second peak 800 Volts. The fact that there is more than one peak in the figure suggests that the switching of all phases was not simultaneous as expected. The fact that there are only two peaks and not three is somewhat unusual. It may be due to the simultaneous closing (arc establishment) of two

of the phases or perhaps one of the phases closed at zero voltage.

Figures 3(b) and 3(c) give a more detailed view of the behavior of the two surges. Both consist of a very fast voltage rise followed by a damped oscillation.

The main oscillation frequencies in both peaks were obtained by applying a Fourier Transform to the data corresponding to both peaks<sup>1</sup>. There is a dominant frequency, located at around 80 kHz, and a secondary one at about 480 kHz. The spectrum exhibits an oscillatory behavior, with a “period” of about 150 kHz.

Other events exhibit a similar behavior.

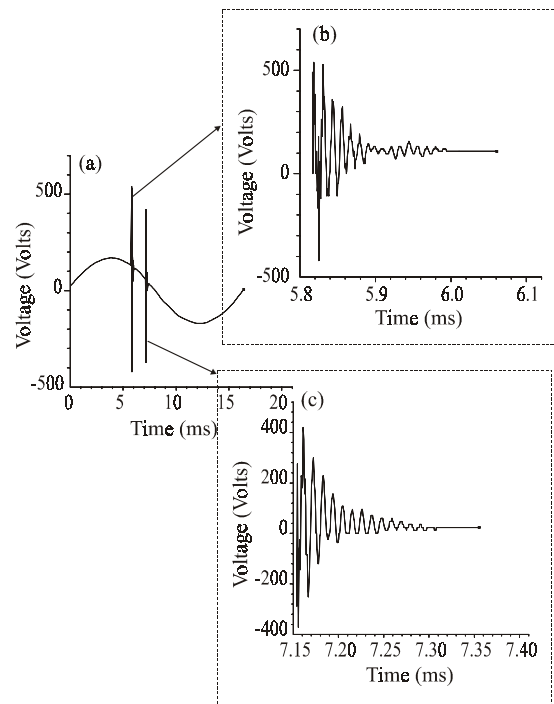


**Figure 3. Voltage Measurements for Event #16 at Point B; (a): Total Event, (b): Close up on First Peak, (c): Close-up on Second Peak.**

## 4. Outline of the Computation Method

### 4.1. Overview

The treatment of switching events in the time domain is usually quite straightforward since switches are devices that can easily be modeled in the time domain, for instance as time-varying resistances. The problem with a time-domain model is that the frequency dependence of various parts of the circuit is difficult to take into account. When using frequency-based programs to model a transient, the frequency dependence of the various components of the network is fully taken into account, but switching is difficult to model. This section describes a simple way to model a switch in the frequency domain through the use of a time-varying voltage source.

It is a general fact that any device in an electrical circuit that has a time-varying voltage drop  $V(t)$  across it can be replaced by a time-varying voltage source with the same voltage without affecting any of the currents and voltages anywhere else in the circuit. This statement is usually not very useful since it requires the computation of the voltage drop across the device, which normally requires solving the whole circuit. The picture is different for an ideal switch, however. In this case, the voltage across the device is equal to the open circuit voltage across it when the switch is open and is equal to zero when the switch is closed. In this way, the full voltage  $V_S(t)$  across the switch can be found from the knowledge of the open-circuit voltage across the switch, a simpler problem that can sometimes be solved. This is then amenable to a frequency-domain treatment by simply taking the Fourier transform of that switch voltage.

Through the superposition principle, any current or voltage anywhere in the circuit (generically denoted by  $Q(t)$ ) can be represented as the sum of two quantities, one due to the switch voltage ( $Q_S(t)$ ) and the other due to other sources in the network ( $Q_E(t)$ , “E” being for external), i.e.

$$Q(t) = Q_S(t) + Q_E(t) \quad (1)$$

where  $Q_S(t)$  is obtained by imposing  $V_S(t)$  across the switch and shorting out all other sources and  $Q_E(t)$  is obtained by shorting out the switch and leaving all other sources at their normal values.

### 4.2. Special Considerations for Harmonic Sources

The strategy outlined above is quite general and could be applied to a wide variety of cases. An important case is when the sources in the network are harmonic at a frequency  $f_0$ . The open-circuit voltage across the switch is then also harmonic at the same frequency and the full

switching voltage  $V_S(t)$  is that same harmonic voltage at all times before the switching time and zero afterwards (the discussion will be limited to a single switch closing event).

Such a waveform for  $V_S(t)$  is somewhat difficult to handle for the Fast Fourier Transform algorithm. Physically, the waveform can extend for several cycles, both before and after the switching event. In fact, a good approximation would be to consider the waveform as extending to infinity in both directions. However, the Fast Fourier Transform can only handle a signal that has a finite extent in time and so the waveform has to be truncated. A naïve way to do this would be to use, say, 5 cycles of the waveform before the switching and the same amount of time after the switching. This would not work correctly, for the following reason.

The Fourier Transform of a harmonic signal is highly concentrated around the harmonic frequency and is oscillating at a “period” of about  $1/T$  where  $T$  is the duration of the harmonic signal. On the other hand, the frequency resolution of a Fourier Transform is  $1/T_F$  where  $T_F$  is the time duration of the signal. If the time duration of the harmonic signal is the same as that of the part which is set at zero,  $T_F$  will be only twice  $T$  which means that only two points per “period” in the frequency domain will be available for the computation of the Fourier integral. This is not enough: at least 6 points should be used, preferably more. Therefore, the duration of the part of the signal that is set to zero (closed switch stimulating the fault) should be at least 5-6 times that of the harmonic signal. In practice, only one cycle (representing the steady-state initial condition) was used while the fault condition duration (closed switch) was 7 times longer.

### 4.3. Computation Tools

To obtain the transient GPR (in the time domain) in the conductor network modeled, a number of representative frequencies are selected from the frequency spectrum of the surge signal and then used to compute the frequency domain responses of the GPR. The inverse Fourier transform is applied to the frequency domain responses to obtain the transient GPR. The computation of the frequency domain responses is carried out using the field theory approach. The HIFREQ and FFTSES engineering modules of the CDEGS software package<sup>2</sup> are used to perform the computations. The HIFREQ module is used to compute the currents and GPR throughout the conductor network in the frequency domain, while the FFTSES module is used for the Fourier transform. The methods used to compute the current distribution and the electromagnetic fields generated by the energized

conductor network are described in Ref. 3 and its references.

#### 4.4. Modeling Steps

From the theoretical considerations above, the following steps can be completed to model switches in the frequency domain.

1. Model the entire conductor network, as shown in Figure 1, in the HIFREQ module, including all desired switches.
2. Obtain the open-circuit voltages across the switches using the HIFREQ module at 60 Hz (steady-state condition).
3. Construct the time-domain voltage waveforms  $V_S(t)$  which appear across the switches, using 1 cycle to simulate the open-circuit voltage (open condition) and seven cycles at zero voltage (close condition). Then, compute the forward FFT of these signals using FFTSES to obtain the frequency-domain voltages across the switches.
4. Short out all switches corresponding to the closed condition after all of switches are closed, use the normal values for the sources' energizations and use the HIFREQ module at 60 Hz to obtain the response  $Q_E(t)$  at the points of interest.
5. Insert a unit energization at one switch location Switch  $S_1$ , short out all other sources and switch locations and carry out a transient analysis using HIFREQ and FFTSES until the spectrum at the points of interest is well defined. Obtain the time-domain results  $Q_{S_1}(t)$  at the points of interest. Repeat for all other switches.
6. To obtain the final response  $Q(t)$  at the points of interest, add the contributions from all switches  $Q_{S_1}(t)$ ,  $Q_{S_2}(t), \dots, Q_{S_N}(t)$ . to the response obtained in Step 4  $Q_E(t)$ .

Note that the Step 6 is valid for  $N$  switches, as long as they are all switched at the same time.

#### 4.5. Verification of Method

The methodology described above has been verified successfully in modeling a switch in a simple series RLC circuit.

### 5. Computation Results

The computation strategy outlined above was applied to the case of Capacitor Bank 5 being switched on, with Capacitor Bank 3 already in service, corresponding to Figure 4. The remaining banks were turned off and were

not modeled. Inset 1 of Figure 4 shows the locations of the three switches.

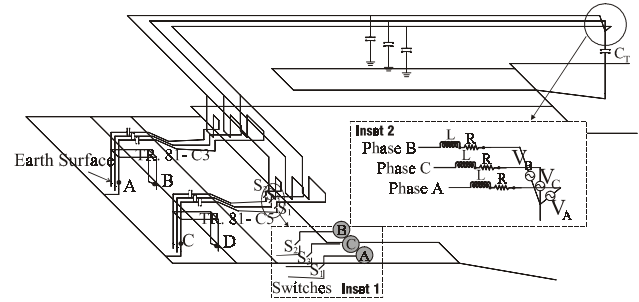


**Figure 4. Switches Modeled in the Network**

Two forms of energization were considered in this study:

- An unbalanced energization at the transformer location.
- A balanced energization at the transformer location.

Inset 2 in Figure 4 shows the energization at the transformer location. The energization parameters for the unbalanced energization are (in V):

$$V_A = 19920.0 e^{j0^\circ}, V_C = 19920.0 e^{j120^\circ}, V_B = 19920.0 e^{-j60^\circ}$$

A very large unbalance is used. This forces currents into the grounding grid and therefore reveals some of its electrical properties. The resonance frequencies of the system should not change for the various energizations; however, the relative amplitudes of the resonances depend greatly on the energization scheme.

#### 5.1. Open-Circuit Voltage Across Switches

As indicated in Figure 4, three switches,  $S_1$  (for Phase A),  $S_2$  (for Phase B) and  $S_3$  (for Phase C) are used to model the switching at Capacitor Bank 81-C5. To obtain the open-circuit voltage at the switch location (Step 2), the conductors near the switches are shortened to create a gap at the switch location. The open-circuit voltages are computed as the GPR differences across the gaps. The open-circuit voltages (peak value) at the switches for both unbalanced energization and balanced energization are listed in Table 1.

**Table 1 Open-Circuit Voltages for Unbalanced Energization and Balanced Energization**

Unbalanced Energization	Balanced Energization
$V_{S_1}^0(t) = 13383.6 \sin(\omega_0 t - 0.2)$	$V_{S_1}^0(t) = 20072.8 \sin(\omega_0 t - 0.2)$
$V_{S_2}^0(t) = 24121.8 \sin(\omega_0 t + 133.7)$	$V_{S_2}^0(t) = 20071.6 \sin(\omega_0 t + 119.8)$
$V_{S_3}^0(t) = 17703.0 \sin(\omega_0 t - 79.3)$	$V_{S_3}^0(t) = 20073.4 \sin(\omega_0 t - 120.2)$

where  $\omega_0 = 2\pi f_0$  and  $f_0$  is the frequency (60 Hz). Following Step 3 in Section 4.4, the time-domain voltages across the switches are constructed; they are displayed in Figure 5, for the unbalanced energization at the transformer.

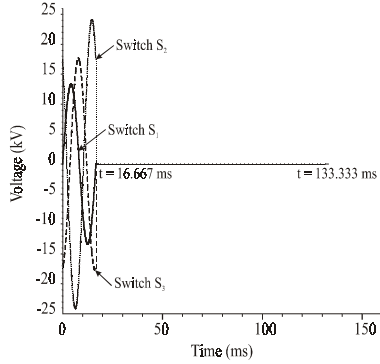


**Figure 5. Time-Domain Voltages Across Switches  $S_1$ ,  $S_2$  and  $S_3$  During Switching at Capacitor Bank 81-C5. Unbalanced Energization Applied at Transformer.**

### 5.2. 60 Hz Response of System $Q_E(t)$

The 60 Hz response of the system is obtained by keeping the three switches closed (Step 4 in Section 4.4). This gives  $Q_E(t)$  of the final time-domain results in Eq. (1). In this study, we are interested in the GPRs near the two capacitor banks (Points A to D in Figure 4). In particular, we are interested in the transient GPR at Point B, in order that a comparison can be made between the present approach and the hybrid approach<sup>1</sup>. The evolution of these quantities in the time domain are given by:

$$Q_E(t) = V_o \sin(\omega_0 t + \phi_o)$$

where  $\omega_0 = 2\pi f_0$  and  $f_0$  is the frequency (60 Hz). For the unbalanced energization,  $V_o = 0.0982$  V and  $\phi_o = -126.6^\circ$ . For the balanced energization,  $V_o = 0.1652$  V and  $\phi_o = -161.1^\circ$ . These values are negligible compared with the transient voltages obtained in the next section.

### 5.3. Transient Response of System $Q_S(t)$ Due to Switching at $S_1$ , $S_2$ and $S_3$

Following Step 5 in Section 4.4, the transient response of the system  $Q_S(t)$  due to switching at TR. 81-C5 can be obtained. Because there are three switches in the system, the total transient response of the system due to switching is the sum of the responses  $Q_{S_1}(t)$ ,  $Q_{S_2}(t)$ , and  $Q_{S_3}(t)$ . The response  $Q_{S_1}(t)$  is due to the switching at  $S_1$ , while  $S_2$  and  $S_3$  are shorted out. The responses  $Q_{S_2}(t)$  and  $Q_{S_3}(t)$  are obtained in the same way.

$$Q_S(t) = Q_{S_1}(t) + Q_{S_2}(t) + Q_{S_3}(t) \quad (2)$$

Figure 6 shows the transient response of the GPR at Point B for the unbalanced energization. The transient GPRs at Points A, C and D are very similar to the results at Point B.

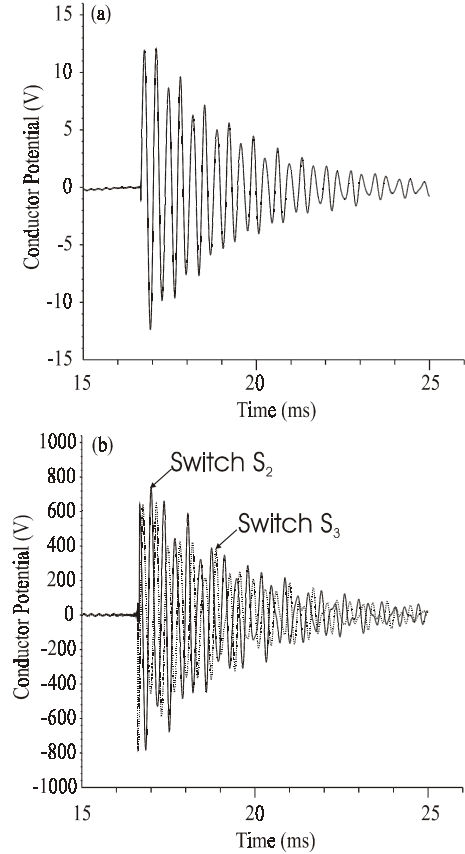


**Figure 6. Switching Transient Voltage at Point B: (a)  $Q_{S_1}(t)$ ; (b)  $Q_{S_2}(t)$  and  $Q_{S_3}(t)$ . Unbalanced Energization is Applied at Transformer.**

Figure 6 indicates that the transient GPR due to Switch  $S_1$  (Figure 6(a)) is much smaller than those due to Switches  $S_2$  and  $S_3$  (Figure 6(b)). As shown in Figure 5, this is because the switching voltage is almost zero when Switch  $S_1$  is closed, while a significant magnitude still remains at the moment when Switches  $S_2$  and  $S_3$  are closed. Furthermore, Figure 6(b) indicates that there is a phase shift between the transient GPR from  $S_2$  and that from  $S_3$ , which leads to a significant cancellation in the total transient voltages at Point B (see next section).

### 5.4. Total Transient Response

The contributions due to the external energizations and those due to the switches must now be added to produce the final result (Step 6 in Section 4.4):

$$Q(t) = Q_E(t) + Q_{S_1}(t) + Q_{S_2}(t) + Q_{S_3}(t) \quad (3)$$

The results are displayed in Figure 7. As compared with the value obtained by the hybrid method (about 1400 V peak-to-peak, Figure 13 in Ref. 1), the magnitude of the overvoltage in Figure 7 is smaller, reaching only about 700 V (peak-to-peak). This value is in better agreement with experimental results (see Figure 3(c)). The steady-state voltage, however, is much smaller than the measured value. This is caused by the mismatch between the computer model and experimental setup (see Section 3). The oscillation frequency of the computed transient GPR is around 3.0 kHz, which is also much smaller than the dominant frequencies in the measurements. The transient voltages at Point B, corresponding to the balanced energization, are almost identical to the ones shown in Figure 7.

It can also be seen from Figures 6 and 7 that the overvoltage at the capacitor bank depends very much on the switching time of the switches. For instance, at Point B, the overvoltages could reach 1600 V (peak-to-peak) if the transient voltages from Switch  $S_2$  and  $S_3$  are in-phase. Several peaks may occur if the switches are closed at different times.

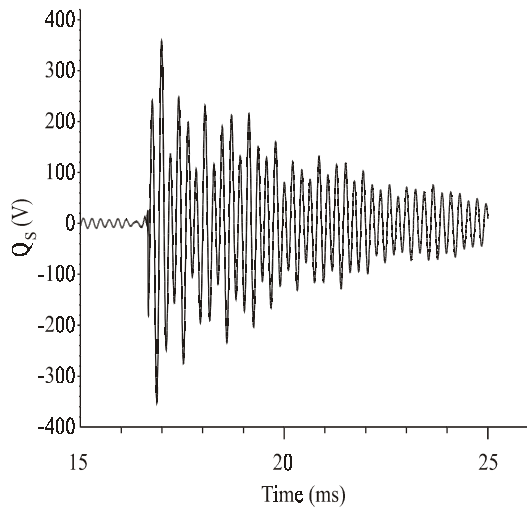


**Figure 7. Total Transient Voltage at Point B. Unbalance Energization Applied at Transformer.**

It is important to note that the portion of the waveforms shown in Figure 7 prior to the switch time are fictitious values and should be ignored. These results are generated due to the aliasing effects from the Fourier Transform. The existence of aliasing effects is due to a finite time period of the open-circuit voltages across the switches (Figure 5, see Section 5.1), while in reality the time both before and after switching should extend to infinity. The responses before the switching are the open-circuit voltages containing purely the 60 Hz steady-state responses.

### 5.5. Frequency Characteristics of the Transient Response at TR.81-C3

Based on the switching transient response shown in Figure 7, it is found that the dominant resonance frequency at capacitor bank TR 84-C3 is around 2.86 kHz. The natural frequency of 2.86 kHz is consistent with the values determined in Ref. 1. The dominant frequencies can be clearly observed in the unmodulated potential at Point B at the capacitor bank TR 84-C3. The unmodulated system response is defined as a response due to a unit energization across the switches. Figure 8 shows the unmodulated potential at Point B due to the closing of Switch  $S_2$ . Although the system exhibits several resonance frequencies, the modulated response (after multiplying the unmodulated potentials by the frequency spectrum of the switching voltage) indicates that the dominant frequency is around 3.0 kHz. Similar patterns can be found at Points A, C and D.

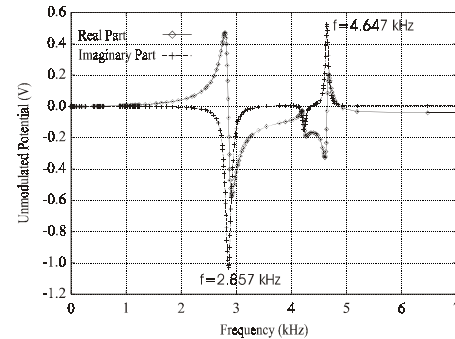


**Figure 8. Unmodulated Potential at Point B.**

## 6. Conclusion

A new technique to model switching operations in the frequency domain using electromagnetic field theory has been developed and applied to study the transient voltages developed due to capacitor bank switching in a system involving both aboveground and buried conductors. The computed transient voltage is smaller than the value obtained by the hybrid method. However, it is in better agreement with measurements.

## 7. References

1. F. P. Dawalibi, S. Fortin, W. Ruan, J. Ma, and S. G. Lodwig, "Analysis of Electric Transients during Capacitor Switching Operations in a Substation", *Proceedings of The 59th American Power Conference*, Chicago, pp. 185-190, April 1997.
2. F. P. Dawalibi and F. Donoso, "Integrated Analysis Software for Grounding, EMF and EMI", *IEEE Computer Applications In Power*, Vol. 6, No. 2, pp. 19-24, 1993.
3. S. Fortin, F. P. Dawalibi, J. Ma, and W. Ruan, "Effects of AC Power Line Configuration and Current Unbalance on Electromagnetic Fields", *Proceedings of The 57th American Power Conference*, Chicago, pp. 170-175, April 1995.